Fabrication and characterization of high-quality-factor silicon nitride nanobeam cavities

Mughees Khan,* Thomas Babinec, Murray W. McCutcheon, Parag Deotare, and Marko Lončar

School of Engineering and Applied Sciences, Harvard University, Cambridge, Massachusetts 02138, USA

**Corresponding author: mkhan@seas.harvard.edu*

Received November 1, 2010; revised December 16, 2010; accepted December 16, 2010; posted January 7, 2011 (Doc. ID 137437); published February 1, 2011

We present the fabrication and characterization of high-quality-factor (Q) Si_3N_4 photonic crystal nanobeam cavities at visible wavelengths for coupling to nitrogen-vacancy centers in a cavity QED system. Confocal microphotoluminescence analysis of the nanobeam cavities demonstrates quality factors up to $Q \sim 55{,}000$, which are limited by the resolution of our grating spectrometer. This is a 1-order-of-magnitude improvement over previous SiN_x cavities at this important wavelength range. We also demonstrate coarse tuning of cavity resonances across 600–700 nm by lithographically scaling the size of fabricated devices.

OCIS codes: 230.5298, 220.4241, 350.4238, 270.0270.

Visible nanophotonics has a wide variety of applications ranging from classical and quantum information processing to compact biological and chemical sensing. One specific example lies in the development of integrated photonic systems with embedded diamond color centers for quantum optics applications. Special emphasis is placed on the nitrogen-vacancy (NV) center as an active element, since it possesses both spin [1] and photon [2] quantum bits for quantum information processing. Recent developments, such as diamond nanowire antennas fabricated from bulk diamond samples [3,4], plasmon-enhanced antennas [5], and optical cavities in other material systems coupled to proximal diamond nanocrystals [6–10], have shown that it is possible to engineer the optical properties (e.g., collection efficiency, radiative rate) of a single NV center. An alternative system that has been shown to theoretically approach the strong-coupling regime of cavity quantum electrodynamics (cQED) is based on coupling the zero-phonon line emission (637 nm) of an NV center in a diamond nanocrystal to a high-quality-factor ($Q \sim 10^5$) silicon nitride (SiN_x) nanobeam cavity [11]. Toward this end, we describe the fabrication and characterization of a high-Q-factor nanobeam photonic crystal (PhC) cavity in an air-bridge Si_3N_4 structure and demonstrate devices with quality factor $Q \sim 55{,}000$, which is limited by the resolution of our measurement. This is 1 order of magnitude higher than previously reported at visible wavelengths [12–16] and approaches the regime necessary for such cQED studies.

In a nanobeam PhC cavity, optical confinement is provided by photonic crystal mirrors along the waveguide dimension and by total internal reflection in the other two transverse dimensions. The cavity design for the devices studied in this work was optimized for a 200-nm-thick, $n = 2.0$ stoichiometric Si_3N_4 device layer. The nanobeam design was 300 nm wide and with a one-dimensional photonic crystal lattice of circular holes with periodicity $a = 250$ nm and radius $r = 70$ nm. The spacing between photonic mirrors was chosen to generate a cavity resonance at 637 nm. To minimize light scattering outside the cavity, the PhC hole mirror was adiabatically tapered [11] by linearly reducing the PhC hole spacing from $a = 250$ nm and hole size $r = 70$ nm in the mirror to $a_0 = 205$ nm and $r_1 = 55$ nm at the cavity center.

Figure 1(a) shows the cavity mode profile for this 4-hole taper cavity, with theoretical quality factor Q = 230,000 and mode volume $V_m = 0.55(\lambda/n)^3$. The cavity Q factor is highly sensitive to the cavity length, defined as the center-to-center distance of the two central holes, and varies by 2 orders of magnitude over a 15 nm range.

A 200-nm-thick high-stress, low-pressure chemical vapor deposition (LPCVD) Si_3N_4 film on a $\langle 100 \rangle$ Si substrate was used in the device layer during fabrication. A Woollam spectroscopic scanning ellipsometer confirmed the refractive index $n \approx 2.0$ of the stoichiometric nitride

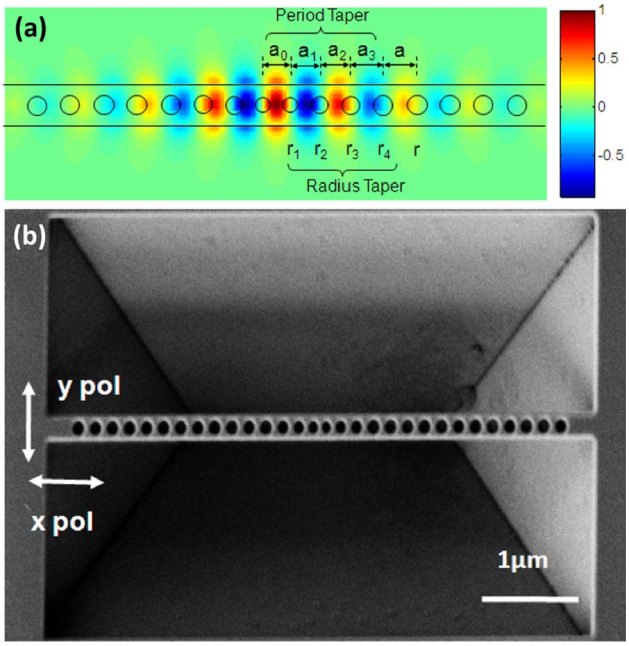

Fig. 1. (Color online) (a) Mode profile (E_y) of a nanobeam photonic crystal cavity with Q = 230,000 and $V_m \sim 0.55(\lambda/n)^3$ based on a four-hole taper with radius, r, and period, a, linearly increasing from 55 to 70 nm and 205 to 250 nm, respectively, in the mirror sections. (b) Fabricated Si_3N_4 cavity with arrows that denote the polarization with respect to the cavity.

0146-9592/11/030421-03$15.00/0

film prior to processing. An approximately 250-nm-thick layer of ZEP 520A or polymethyl methacrylate (PMMA 950C3) was used as electron beam resist, which was spun at 4000 rpm for 40 s and then soft baked at 180 °C for 2 min and 3 min, respectively. PMMA showed better adhesion to Si_3N_4 compared to ZEP, though oxygen plasma cleaning was observed to improve ZEP adhesion. An ELS-7000 (Elionix Inc., Japan) 100 KV electron beam lithography tool was used to pattern the designed four-hole tapered PhC nanobeam structure in the resist. The ZEP-coated samples were developed in o-xylene for 120 s, and the PMMA-coated samples were developed in a 1∶3 mixture of methyl isobutyl ketone (MIBK): isopropyl alcohol (IPA) for 90 s. After development, the patterned PhC structure was transferred to the Si_3N_4 film in a reactive ion etcher (RIE) using a $C_4F_8/SF_6/H_2$ recipe in an inductively coupled reactive ion etcher at 120 nm/ min Si_3N_4 etch rate with smooth, near-vertical sidewalls. After stripping the resist in acetone, KOH:H_2O (1∶4) solution [17,18] was used to etch the exposed Si at 65 °C. KOH:H_2O also stripped any remaining ZEP. Potassium hydroxide (KOH) selectivity to different Si planes was considered as part of the fabrication process and allowed the successful release of the air-bridge PhC cavity [Fig. 1(b)]. The presence of a highly stressed Si_3N_4 film allowed releasing of the air-bridged cavity using wet isotropic etching of Si without the use of any critical point drying to release the suspended structures. However, stresses in the LPCVD Si_3N_4 film may have caused preferential KOH etching of Si_3N_4 around the air holes, making them slightly elliptical.

A home-built microphotoluminescence system was used to characterize the photonic crystal nanobeam cavities [Fig. 2(a)]. The nanobeam photonic crystals were pumped with ~500 μW of a 532 nm CW laser using a 0.95 NA objective, and a three-axis piezoelectric stage scanned the sample stage underneath the pump beam. Low-level, intrinsic fluorescence was collected back through the objective and focused on a 1×2 single-mode fiber beam splitter acting as a confocal pinhole. One arm

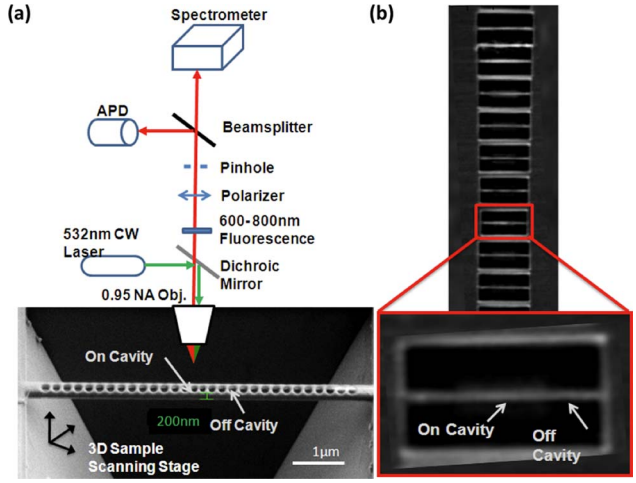

Fig. 2. (Color online) (a) Cartoon of the confocal microscope used in this experiment. (b) 2D confocal microscope image showing an array of cavities having different scaling percentages separated by spacers. Inset, zoomed-in image of one cavity.

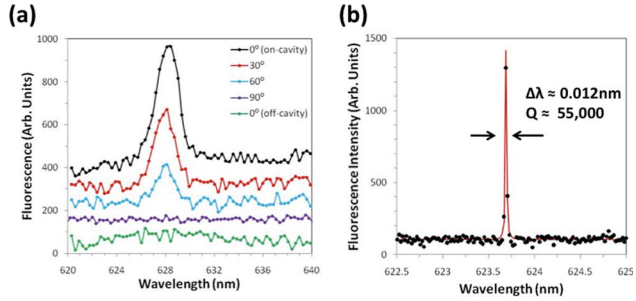

Fig. 3. (Color online) (a) Cavity resonance as a function of polarization measured with a coarse 150 l/mm grating, (b) cavity resonance measured with a high-resolution 1800 l/mm grating. Data (black circles) and Lorentzian fit (red line) gives $Q \sim 55{,}000$.

of the beam splitter was connected to an avalanche photodiode to generate an image of the sample and optically address individual nanobeam devices [Fig. 2(b)]. The second arm of the beam splitter was connected to a spectrometer in order to confirm the presence of individual resonant features in the cavity fluorescence. For example, a linear polarizer in the collection path showed high transmission of the cavity signal when parallel to the cavity dipole [Fig. 3(a), black] and extinction for the orthogonal direction [Fig. 3(a), purple]. Moreover, the cavity signal was observed to vanish when taking photoluminescence spectra several spot sizes ~1–2 μm away from the cavity center due to its small mode volume [Fig. 3(a), green]. At this stage, measurements of the cavity spectrum were artificially broadened due to the low-resolution (150 l/mm) grating.

The quality factors $Q = \lambda/\Delta\lambda$ of these resonances were then measured with a high-resolution grating (~1800 lines/mm) and fitting to a Lorentzian profile. Devices were routinely observed with $Q > 10^4$, and the best device that we characterized possessed a quality factor $Q = 5.5 \pm 1.0 \times 10^4$ [Fig. 3(b)]. The large uncertainty in Q in this case results from the fact that the width $\Delta\lambda$ of this device resonance is comparable to the resolution limit of our grating spectrometer. Some devices demonstrated even narrower resonances (data not shown), but with few (<3) points so that the cavity Q factor is potentially larger but also difficult to fit reliably. An important observation was the difficulty in characterizing cavities with an ultrahigh Q factor due to low fluorescence counts. To overcome fabrication tolerances and generate a coarse tuning mechanism to couple these narrow cavity resonances to emitters with likewise narrow emission profiles, we scaled the nanobeam device parameters at a fixed value of r/a in order to shift the resonant wavelength. The result, which is shown in Fig. 4, shows good agreement between simulated and measured device wavelengths for cavities with $(-2, +2, +5, +10)\%$ scaling.

In this Letter we have presented the design, fabrication, and characterization of silicon nitride nanobeam cavities at visible wavelengths. By utilizing a four-hole taper design, devices with $Q \sim 55{,}000$ and approaching 10^5 were observed using μPL measurements. Additional characterization of the resonances in these devices with more sensitive detection schemes, for example, based on a fiber-taper probe [19] or resonant scattering [20], could

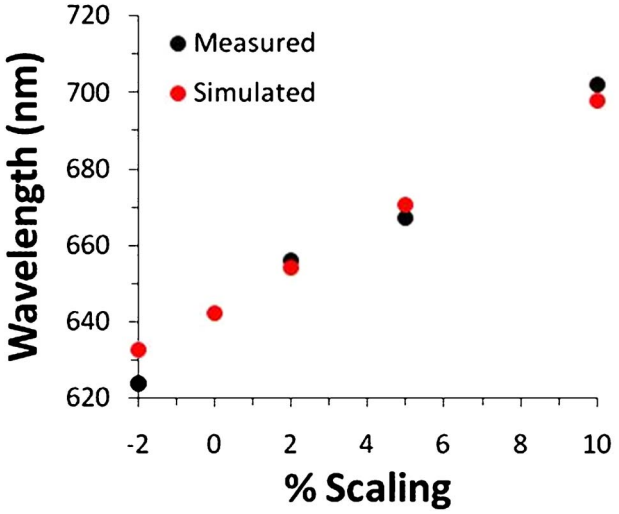

Fig. 4. (Color online) Comparison between experimental and theoretical data for nanobeam cavities that are scaled versions of the optimal design.

allow for the observation of even higher Q modes beyond the level observed here. Moreover, the introduction of light emitters such as diamond color centers, for example, using deterministic AFM-coupling techniques [8,10], will allow us to investigate cQED phenomena.

The authors thank the National Science Foundation (NSF) under Nanoscale Interdisciplinary Research Team (NIRT) grant ECCS-0708905 and Harvard's National Science and Engineering Center (http://www.nsec.harvard.edu) for financial support. M. W. McCutcheon kindly thanks the Natural Science and Engineering Research Council of Canada (NSERC) for its generous support. T. Babinec was funded by the National Defense Science and Engineering Graduate (NDSEG) graduate student fellowship. Most of the nanofabrication work was performed at Center for Nanoscale (CNS) at Harvard University. The authors would also like to thank the CNS staff members, especially Dr. Ling Xie and Steve Paolini for their help and support.

References

1. F. Jelezko, T. Gaebel, I. Popa, A. Gruber, and J. Wrachtrup, Phys. Rev. Lett. **92**, 076401 (2004).
2. A. Beveratos, R. Brouri, T. Gacoin, J.-P. Poizat, and P. Grangier, Phys. Rev. A **64**, 061802(R) (2001).
3. T. M. Babinec, B. J. M. Hausmann, M. Khan, Y. Zhang, J. R. Maze, P. R. Hemmer, and M. Loncar, Nat. Nanotechnol. **5**, 195 (2010).
4. B. J. M. Hausmann, M. Khan, Y. Zhang, T. Babinec, K. Martinick, M. McCutcheon, P. R. Hemmer, and M. Loncar, Diam. Relat. Mater. **19**, 621 (2010).
5. S. Schietinger, M. Barth, T. Aichele, and O. Benson, Nano Lett. **9**, 1694 (2009).
6. P. E. Barclay, C. Santori, K.-M. Fu, R. G. Beausoleil, and O. Painter, Opt. Express **17**, 8081 (2009).
7. D. Englund, B. Shields, K. Rivoire, F. Hatami, J. Vuckovic, H. Park, and M. D. Lukin, Nano Lett. **10**, 3922 (2010).
8. M. Barth, N. Nuesse, B. Loechel, and O. Benson, Opt. Lett. **34**, 1108 (2009).
9. Y.-S. Park, A. K. Cook, and H. Wang, Nano Lett. **6**, 2075 (2006).
10. T. van der Sar, J. Hagemeier, W. Pfaff, E. C. Heeres, T. H. Oosterkamp, D. Bouwmeester, and R. Hanson, http://eprintweb.org/s/article/quant-ph/1008.4097 (2010).
11. M. W. McCutcheon and M. Lončar, Opt. Express **16**, 19136 (2008).
12. M. Makarova, J. Vuckovic, H. Sanda, and Y. Nishi, Appl. Phys. Lett. **89**, 221101 (2006).
13. M. Barth, J. Kouba, J. Stingl, B. Loechel, and O. Benson, Opt. Express **15**, 17231 (2007).
14. M. Barth, N. Nuesse, J. Stingl, B. Loechel, and O. Benson, Appl. Phys. Lett. **93**, 021112 (2008).
15. Y. Gong and J. Vuckovic, Appl. Phys. Lett. **96**, 031107 (2010).
16. K. Rivoire, A. Faraon, and J. Vuckovic, Appl. Phys. Lett. **93**, 063103 (2008).
17. H. Seidel, L. Csepregi, A. Heuberger, and H. Baumgarel, J. Electrochem. Soc. **137**, 3612 (1990).
18. D. Kendall, Annu. Rev. Mater. Sci. **9**, 373 (1979).
19. K. Srinivasan, P. E. Barclay, M. Borselli, and O. Painter, Phys. Rev. B **70**, 081306(R) (2004).
20. P. B. Deotare, M. W. McCutcheon, I. W. Frank, M. Khan, and M. Loncar, Appl. Phys. Lett. **94**, 121106 (2009).